

# A New Approach to Background Subtraction in Low-Energy Neutrino Experiments

Y-F. Wang, L. Miller, G. Gratta

Physics Department, Stanford University, Stanford CA 94305

(November 4, 2018)

We discuss a new method to extract neutrino signals in low energy experiments. In this scheme the symmetric nature of most backgrounds allows for direct cancellation from data. The application of this technique to the Palo Verde reactor neutrino oscillation experiment allowed us to reduce the measurement errors on the anti-neutrino flux from  $\sim 20\%$  to  $\sim 10\%$ . We expect this method to substantially improve the data quality in future low background experiments such as KamLAND and LENS.

PACS 14.60.Lm, 14.60.Pq, 29.85.+c

## I. INTRODUCTION

Backgrounds are a major concern in low-energy neutrino experiments where signals have low rates and are easily mimicked by other phenomena. Several types of coincidence schemes, specific to particular neutrino-induced processes, have been proposed to improve the signal-to-noise ratio. One classic example is the use of the inverse- $\beta$  decay process

$$\bar{\nu}_e + p \longrightarrow e^+ + n \quad (1)$$

in liquid scintillator in the discovery of neutrinos and many subsequent experiments [1,2]. Positrons deposit their energy in the scintillator and annihilate, yielding two 511 keV  $\gamma$ 's. Neutrons are captured after thermalization, producing  $\gamma$ 's. The two parts of the event are separated in time by a delay ranging from tens to hundreds of microseconds depending upon the nucleus on which the neutron captures. The use of similar time correlations has been proposed for solar neutrino detection [3].

It is often the case that experiments are still background limited even when such coincidence schemes are adopted, particularly when the signal rate is very low and can not be varied. Using data from the Palo Verde neutrino oscillation experiment [4], we have found that most backgrounds have a peculiar symmetry in the energy depositions between the two parts of an event that is not present in the neutrino signal. Such symmetry allows one to eliminate most of the background by direct subtraction with the data itself.

In this paper we discuss in detail the method using the data from the Palo Verde experiment as an example and its application to future experiments such as KamLAND [5] and LENS [3], where signal rates are expected to be substantially lower.

## II. BACKGROUNDS TO REACTOR NEUTRINO EXPERIMENTS

Low-energy electron anti-neutrinos from nuclear reactors are unique tools to study oscillations in the regime

of large mixing angle and small mass differences. Such combination of parameters has recently received a good deal of attention as it is consistent with a number of observations involving solar and atmospheric neutrinos [6]. In recent times two experiments of this type [4,7] have been set up to search for  $\bar{\nu}_e - \bar{\nu}_x$  oscillations compatible with the atmospheric neutrino anomaly. In these experiments, electron anti-neutrinos from reactors with energies less than 10 MeV, are detected by the reaction (1) in liquid scintillator. There are two types of backgrounds to this process: uncorrelated background from environmental radioactivity randomly occurring during the time coincidence window, and correlated background from cosmic-muon-induced fast neutrons. While the first one can be easily measured by varying the time correlation window, the second one is more difficult to be measured unambiguously. Neutrons discussed here are produced either in the laboratory walls or inside the detector. Michel electrons from muon decays are not a background since their time correlation is short and their energy deposition too large.

Fast neutrons can mimic the anti-neutrino signal in the following two ways:

- *one-neutron background*: A proton recoil is produced through a fast-neutron scattering mimicking the  $e^+$  signature; the neutron is then thermalized and captured like in the case of anti-neutrino events.
- *two-neutron background*: The fast neutron can produce a secondary neutron through a spallation process on nuclei; both neutrons are then captured simulating the two parts of an anti-neutrino event.

Both backgrounds are very difficult to measure except in the case when the  $\bar{\nu}_e$  source (in this case nuclear reactors) can be turned off, hence eliminating the signal. This favorable circumstance was available only to the Chooz experiment [7]. Generally, theoretical models describing neutron production are not considered accurate enough to provide a viable tool for background subtraction.

Fast neutrons are produced mainly in muon capture and muon spallation. While the first process is well understood, the second is poorly known. Although the total neutron yield from muon spallation has been, to some extent, experimentally measured [8,9], theoretical models [10–12] are not consistent with each other and with data. In addition the few measurements of the neutron energy spectrum [13] are not well reproduced by theoretical calculations [14,15]. The interpretation of experimental data is complicated by the fact that the neutron energy spectrum depends upon the muon spectrum that, in turn, is a function of the depth at which the measurement was carried-on.

Since modern reactor neutrino oscillation experiments typically have long baselines and observe anti-neutrinos from more than one reactor, in most cases it is impossible to completely turn off the signal source. Hence many experiments rely on the power variations that generally occur during refueling of some of the reactors in order to subtract backgrounds. This method, here referred to as “ON-OFF method”, has serious limitations since: a) the statistical error is large as only a small fraction of the neutrinos are used as signal while most of them are subtracted away with the background; the smaller the power excursion the larger the statistical error; b) since reactors are kept to full power for a very large fraction of time (because of obvious economic reasons) statistical errors are dominated by the short low power periods while the majority of the data taken by the experiment is not useful to improve the measurement accuracy; c) the subtraction method only works under the assumption that backgrounds are stable over the periods of several months that separate the full-power periods from the low-power ones; d) complete systematic checks on data can only be done after an entire reactor cycle that generally corresponds to a period of six months to one year.

The new technique, that we call the “swap method”, avoids such limitations.

### III. THE SWAP METHOD

The swap method uses symmetries of the data to directly eliminate most of the backgrounds and a Monte Carlo calculation to estimate the residual background. The same symmetries that guarantee the cancellation in data also make the whole process rather insensitive to imperfections of the Monte Carlo model.

We first select neutrino events by requiring the prompt part as positron-like and the delayed part as neutron-like. We have:

$$N_1 = B_{\text{unc}} + B_{\text{nn}} + B_{\text{pn}} + N_\nu \quad (2)$$

where  $N_1$  is the number of selected events,  $B_{\text{unc}}$  the uncorrelated background from natural radioactivity,  $B_{\text{nn}}$

the correlated background from two-neutron captures,  $B_{\text{pn}}$  the correlated background from single-neutron-induced events and  $N_\nu$  the anti-neutrino signal to be measured. We then reverse the selection by imposing neutron cuts on the prompt part and positron cuts on the delayed part, obtaining:

$$N_2 = B'_{\text{unc}} + B'_{\text{nn}} + \epsilon_1 B_{\text{pn}} + \epsilon_2 N_\nu \quad (3)$$

Since both uncorrelated and two-neutron backgrounds are symmetric under this selection swap, we have  $B'_{\text{unc}} = B_{\text{unc}}$  and  $B'_{\text{nn}} = B_{\text{nn}}$ . Indeed both  $B'_{\text{unc}}$  and  $B_{\text{unc}}$  can be measured independently and are found to be the same in Palo Verde data. The terms  $B_{\text{pn}}$  and  $N_\nu$  are not *a priori* symmetric and we use the factors  $\epsilon_1$  and  $\epsilon_2$  to describe the efficiencies for the swapped selection.

It is essential to realize here that this procedure can only be applied if the trigger system treats the two parts of the event in an identical fashion. At Palo Verde the symmetric trigger conditions used [16] were found to have an efficiency very similar to the one that would be obtained by separately optimizing the patterns for the positron and the neutron parts of the events.

We can now calculate the difference

$$N_1 - N_2 = (1 - \epsilon_1)B_{\text{pn}} + (1 - \epsilon_2)N_\nu \quad (4)$$

where  $B_{\text{unc}}$  and  $B_{\text{nn}}$  have been eliminated and  $\epsilon_2$  can be easily obtained from the  $\bar{\nu}_e$  Monte Carlo simulation since this process is well known. The derivation of  $\epsilon_1$  is more involved since, as already discussed, the neutron background is not easy to model. Here we remark, however, that the “swap method” owes its power to the fact that, as it will be shown later,  $\epsilon_1 \sim 1$  and  $\epsilon_2 \sim 0$ . A small  $(1 - \epsilon_1)$  relaxes the accuracy requirements on the Monte Carlo simulation to be used to estimate  $(1 - \epsilon_1)B_{\text{pn}}$ .

The Palo Verde detector [17] is shown in Fig. 1. All our simulations use the Monte Carlo program GEANT [18] to describe the detector and the materials surrounding it. Electromagnetic interactions are simulated by GEANT while hadronic interactions are simulated by GFLUKA [19]. Low energy neutron transport is simulated by GCALEOR [20]. Cuts for tracking neutrons are set to 1 MeV for concrete and earth, 100 keV for the veto scintillator, 10 keV for the water shielding and  $10^{-5}$  eV for the central detector. Light quenching for protons in liquid scintillator is also included [21]. Our program successfully simulates the behavior of neutrons from Am-Be and  $e^+$  and  $\gamma$ 's from  $^{22}\text{Na}$  sources, which proves that neutrino signals are simulated correctly [17].

In estimating  $B_{\text{pn}}$  we consider both the process of muon spallation and capture. Each process may happen either in the laboratory walls or inside the boundaries of the veto system. Our selection cuts for the positron part of the  $\bar{\nu}_e$  event have been found to have negligible efficiency for muon-induced radioactivity, so that this

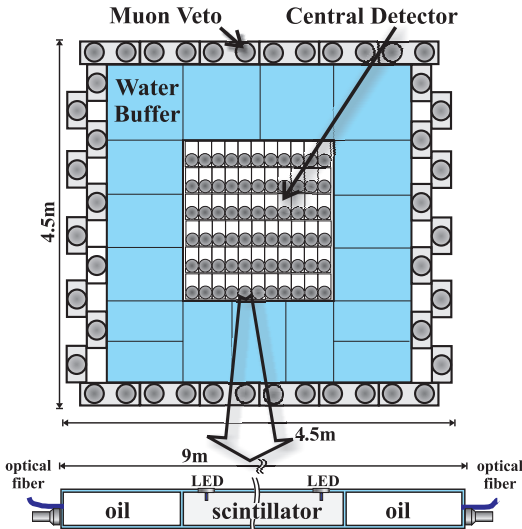


FIG. 1. Schematic view of the Palo Verde neutrino detector. The liquid scintillator is loaded with 0.1% Gd in order to reduce the neutron capture time to 30  $\mu$ s and provide a large capture signal (8 MeV  $\gamma$  cascade).

phenomenon represents a negligible fraction of the background and is not analyzed further. Neutrons from other processes such as neutrino interactions with the rock, photo-nuclear reactions associated with electromagnetic showers generated by muons, and muon elastic scattering, are also found to be negligible.

### A. Muon spallation inside laboratory walls

As it turns out, muon spallation in the concrete walls of the laboratory is the dominant component of  $B_{\text{pn}}$  in the case of Palo Verde. Although absolute rate predictions are not particularly reliable, in our case a normalization point can be obtained from data where the prompt part of the event has an energy in excess of 10 MeV. In fact, above this energy there is no anti-neutrino signal or neutron capture but only proton recoils from neutron collisions. So we use the simulation only to obtain the ratio

$$r = \frac{B_{\text{pn}}^{\text{MC}}(E < 8 \text{ MeV})}{B_{\text{pn}}^{\text{MC}}(E > 10 \text{ MeV})} \quad (5)$$

and then find  $B_{\text{pn}}$  normalizing to data:

$$B_{\text{pn}} = r \cdot B_{\text{pn}}^{\text{data}}(E > 10 \text{ MeV}). \quad (6)$$

We then determine  $(1 - \epsilon_1)r$  using the Monte Carlo simulation.

As mentioned above, the energy spectrum of neutrons from muon spallation is not very well known and a broad range of results can be found in the literature. Barton [14] suggested that the spectrum of neutrons from hadronic cascade follows  $E^{-1/2}$  between 10-50 MeV, while the spectrum of neutrons from  $\pi^-$  capture follows

a flat spectrum up to 100 MeV. Perkins [15] suggested that the neutron spectrum from muon spallation follows  $E^{-1.6}$ . The combination of  $(9.7E^{-1/2} + 6.0e^{-E/10})$  has been used in a measurement [9] at a shallow site. It has also been suggested [22] to use proton and neutron spectra following  $E^{-1.86}$  as measured at accelerators for photo-nuclear interactions. Finally the Karmen experiment reported a visible energy spectrum following  $e^{-E/39}$  for spallation neutrons [13].

We conservatively choose four spectra, including all the options described, as input to our Monte Carlo calculation of backgrounds. Tab. I shows the two extreme cases of  $E^{-0.5}$  and  $E^{-2.0}$  together with the exponential spectrum  $e^{-E/39}$  (Models A). We assume that neutrons are produced isotropically. In addition we compute the neutron spectrum by producing cosmic muons in the energy range  $0.01 \text{ MeV} < E_{\mu} < 500 \text{ GeV}$  according to the proper energy and angular distributions [24]. We then generate real bremsstrahlung  $\gamma$ 's according to the distribution  $1/E_{\gamma}$  in the energy range  $10 \text{ MeV} < E_{\gamma} < E_{\mu}$ . Neutrons are then produced from photo-nuclear processes with a spectral shape  $E^{-1.86}$  [22] and an angular distribution from [23] in the energy range  $10 \text{ MeV} < E_n < E_{\gamma}$ . The result of this method is also reported in Tab. I as Model B.

Model	$\epsilon_1$	$r$	$(1 - \epsilon_1)r$	$B_{\text{pn}}^{\text{MC}}(\text{d}^{-1})$ $E > 10 \text{ MeV}$
$E^{-0.5}$ , A	$1.16 \pm 0.07$	$0.69 \pm 0.04$	$-0.11 \pm 0.05$	155
$E^{-2.0}$ , A	$1.20 \pm 0.11$	$0.67 \pm 0.07$	$-0.13 \pm 0.07$	1.7
$e^{-E/39}$ , A	$1.06 \pm 0.07$	$0.77 \pm 0.05$	$-0.05 \pm 0.06$	17
$E^{-1.86}$ , B	$1.15 \pm 0.06$	$0.76 \pm 0.04$	$-0.11 \pm 0.04$	32
Average			$-0.10 \pm 0.05$	

TABLE I. Results of Monte Carlo simulation for neutrons produced in the laboratory walls by muon spallation. The errors shown are due to limited Monte Carlo statistics. The estimated background rate above 10 MeV shown in the last column refers to an independent calculation, described in the text. The values of  $B_{\text{pn}}^{\text{MC}}(E > 10 \text{ MeV})$  should be compared with a total rate of  $13.5 \pm 0.4 \text{ d}^{-1}$  obtained from Palo Verde data. The differences between Models are discussed in the text.

In order to obtain the results in Tab. I, we use only interactions in a 1 m thick concrete shell as neutrons produced at larger depths are completely absorbed. The 10 MeV low-energy cutoff used in the calculations is justified by the fact that softer neutrons are completely absorbed by the 1 m thick water buffer surrounding the Palo Verde central detector. From Tab. I we can see that the proton-recoil energy is only weakly dependent upon the neutron energy so that both  $\epsilon_1$  and  $r$  remain almost constant for drastically different neutron energy

spectra. Furthermore, the uncertainties on  $\epsilon_1$  and  $r$  have little effect on the factor  $(1 - \epsilon_1)r$  that directly enters the neutrino measurement. This implies that the neutron-capture signal, common to both the neutrino signal and the  $B_{\text{pn}}$  background, is similar to the proton-recoil signal of the background, but different from the positron signal of a neutrino event.

In Fig. 2 we show the energy deposited by the neutron-induced proton recoil in the most energetic cell of the prompt part of the events. The four different neutron spectra used are normalized to data for energies above 10 MeV.

To verify the results obtained we independently calculate the spallation background by using a neutron yield of  $6 \times 10^{-5} \mu^{-1} \text{g}^{-1} \text{cm}^2$  for normalization. This number is obtained by rescaling the measurements of [9] to our depth of 32 m.w.e. A total of  $7.8 \times 10^6$  neutrons are generated daily in our lab walls. The calculated background rates  $B_{\text{pn}}^{\text{MC}}(E > 10 \text{ MeV})$  are shown in the last column of Tab. I, which can be compared with our measurement  $B_{\text{pn}}^{\text{data}}(E > 10 \text{ MeV}) = 13.5 \pm 0.4(\text{stat.}) \text{ d}^{-1}$ . It is clear that our measurement falls somewhere in the middle of the predictions and the spectra chosen for the simulation cover a conservative range of possibilities. We conservatively maintain all four options and use the possible differences as contributions to the systematic errors.

Finally we average  $(1 - \epsilon_1)r$  from Tab. I obtaining  $-0.10 \pm 0.05$ , and then proceed to calculate the background from neutron spallation in the walls as  $(1 - \epsilon_1)B_{\text{pn}} = 1.35 \pm 0.68 \text{ d}^{-1}$ .

### B. Muon spallation inside the veto system

Inefficiencies of the cosmic-ray veto system result in a component of  $B_{\text{pn}}$  from neutrons produced within the detector. The veto inefficiency at Palo Verde is measured to be  $(0.07 \pm 0.02)\%$  for through-going muons (two missed hits). Only neutrons produced in the water buffer are important here since muons responsible for neutron spallation directly in the central detector scintillator would be easily detected and discarded.

Using the same procedure as above we obtain a neutron yield of  $1600 \text{ d}^{-1}$  from the water buffer. The corresponding  $\epsilon_1$ ,  $r$  and  $(1 - \epsilon_1)r$  are given in Tab. II together with background estimates  $B_{\text{pn}}^{\text{MC}}(E > 10 \text{ MeV})$ . It can be readily seen from the Table that  $B_{\text{pn}}^{\text{MC}}(E > 10 \text{ MeV})$  in the water buffer has a negligible rate compared to that in Tab. I, and their  $(1 - \epsilon_1)r$  are very similar. Hence in the rest of our calculations we will neglect this contribution.

### C. Muon capture inside laboratory walls

The muon capture process is rather well understood and the resulting neutrons tend to have a soft spectrum

Model	$\epsilon_1$	$r$	$(1 - \epsilon_1)r$	$B_{\text{pn}}^{\text{MC}} (\text{d}^{-1})$ $E > 10 \text{ MeV}$
$E^{-0.5}$ , A	$1.17 \pm 0.12$	$0.72 \pm 0.07$	$-0.12 \pm 0.08$	2.2
$E^{-2.0}$ , A	$0.94 \pm 0.08$	$1.41 \pm 0.15$	$0.08 \pm 0.11$	0.06
$e^{-E/39}$ , A	$0.97 \pm 0.04$	$1.12 \pm 0.05$	$0.03 \pm 0.04$	0.8
$E^{-1.86}$ , B	$1.13 \pm 0.05$	$1.12 \pm 0.05$	$-0.15 \pm 0.06$	0.9

TABLE II. Results of Monte Carlo simulation for neutrons produced in the water buffer by muon spallation. The errors shown are due to limited Monte Carlo statistics. The estimated rate above 10 MeV shown in the last column refers to an independent calculation, described in the text. It is clear that the rates found for this channel are negligible with respect to the rates in Tab. I.

(compared to spallation), with an upper limit around 100 MeV (muon mass). The underground laboratory at Palo Verde is built with low activity concrete using dolomite as aggregate. The elemental composition of concrete is shown in Tab. III together with the muon capture rate and the neutron yield per capture for each element. Almost every capture produces one neutron. The total un-vetoed muon rate in the walls is 2 kHz, of which 0.9 kHz is due to  $\mu^-$ . The stopping  $\mu^-$  rate amounts to 90 Hz. Using Tab. III we obtain a total muon capture probability of 67%, resulting a neutron production rate of 60 Hz in the laboratory walls.

Element	Fraction by mass (%)	Capture rate ( $10^5 \text{ s}^{-1}$ )	n yield/capture ( $\mu\text{-capture}^{-1}$ )
H	0.6	0.004 [25]	1
C	10.4	0.388 [25]	$\sim 1$ [26]
O	50.6	1.026 [25]	0.98 [26]
Al	0.3	7.054 [25]	1.26 [27]
Si	1.2	8.712 [25]	0.86 [27]
Mg	10.7	10.67 [25]	1 *
Ca	22.9	25.57 [25]	0.75 [27]
Fe	3.3	44.11 [25]	1.12 [27]

\*actual value not known, assumed to be 1

TABLE III. Elemental composition together with muon capture rates and neutron yields for the Palo Verde concrete. The concrete contains 3% reinforcing steel, 16% cement and 81% crushed dolomite aggregate.

The neutron energy spectrum from capture is simulated taking into account both the soft neutrons from nuclear evaporation and the hard neutrons from direct emission. For light elements such as  $^{12}\text{C}$  and  $^{16}\text{O}$ , individual lines are present in the neutron spectrum [28,29], while for heavier elements such spectrum has the properties of a continuum. We use the energy spectra in ref. [28]

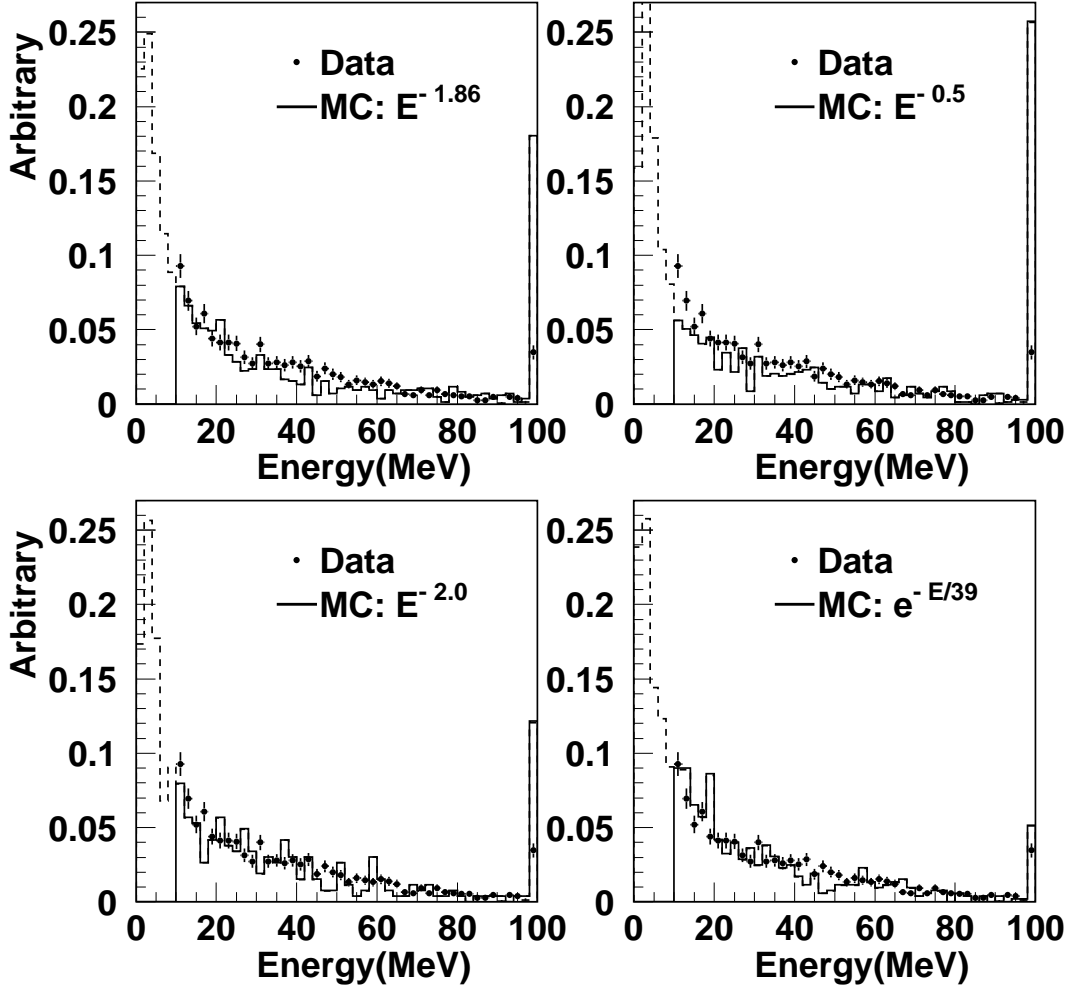


FIG. 2. Energy deposited in the most energetic cell for different neutron spectra. Data and Monte Carlo total rates are normalized above 10 MeV where there is no  $\bar{\nu}_e$  signal in the data. The dashed line is the MC prediction for  $E < 10$  MeV.

to simulate neutrons from  $^{12}\text{C}$  and  $^{16}\text{O}$ , while those from heavy elements are simulated according to [27]. Capture on hydrogen happens at a negligible rate and is disregarded here. From the simulation, we obtain  $B_{\text{pn}} = 0.10 \pm 0.05 \text{ d}^{-1}$  and  $(1 - \epsilon_1) = 0.23 \pm 0.32$  so that  $(1 - \epsilon_1)B_{\text{pn}} = 0.02 \pm 0.03 \text{ d}^{-1}$  where the error includes Monte Carlo statistics and all systematic uncertainties. We conclude that this background is negligible compared to other channels.

#### D. Muon capture inside the veto system

In analogy to the spallation case, neutrons from muon capture inside the veto system can contribute to  $B_{\text{pn}}$  for un-tagged muons. Even considering the conclusions from

the previous two sections this background cannot be a priori dismissed as negligible since the veto counter inefficiency for single hits (such as would result from a stopping muon) is measured to be  $(4 \pm 1)\%$ . In the buffer-water muon capture on  $^{16}\text{O}$  is the only significant source of neutrons since the capture rate on hydrogen is very small.

The total  $\mu^-$  rate in our detector is about 860 Hz, of which 86 Hz are stopping muons. This results in a rate of un-tagged neutrons of  $52500 \text{ d}^{-1}$ . Using the energy spectrum from ref. [28], we obtain from Monte Carlo simulation  $B_{\text{pn}} = 3.9 \pm 0.8 \text{ d}^{-1}$  and  $(1 - \epsilon_1) = 0.22 \pm 0.03$ . Finally, this background contributes  $(1 - \epsilon_1)B_{\text{pn}} = 0.86 \pm 0.50 \text{ d}^{-1}$  where, as usual, the error includes all uncertainties.

	Rate (d <sup>-1</sup> )
$(1 - \epsilon_1)B_{\text{pn}}$ (Spallation in walls)	$0.19 \pm 0.26$
$(1 - \epsilon_1)B_{\text{pn}}$ (Spallation in detector)	-
$(1 - \epsilon_1)B_{\text{pn}}$ (Capture in walls)	-
$(1 - \epsilon_1)B_{\text{pn}}$ (Capture in detector)	$-0.08 \pm 0.08$
Total $(1 - \epsilon_1)B_{\text{pn}}$ (MC)	$0.11 \pm 0.27$
$N_1$ (Data)	$8.75 \pm 0.28$
$N_2$ (Data)	$9.07 \pm 0.29$
$N_1 - N_2$ (Data)	$-0.32 \pm 0.20$

TABLE IV. Comparison of data and Monte Carlo for an event selection with no efficiency for the anti-neutrino signal (see text). Errors are statistical only. Note that  $N_1$  and  $N_2$  are correlated.

### E. Verification of the method

In summary, all the above backgrounds add to a total rate  $(1 - \epsilon_1)B_{\text{pn}} = 0.5 \pm 0.8 \text{ d}^{-1}$ , very close to 0. The error is dominated by systematics, particularly stemming from uncertainties in the neutron energy spectrum.

In order to verify the correctness of the method, we can directly measure in the data a similar background by slightly modifying the anti-neutrino selection cuts so that no signal is detected. Positrons (from  $\bar{\nu}_e$  interactions) differ from proton recoils (from background neutrons interactions) by the annihilation  $\gamma$ 's with energies of less than 511 keV. An event selection requiring more than 600 keV for each of the hits will result in the total rejection of the neutrino signal. Hence in this case only the  $B_{\text{pn}}$  term will be present after swap selection:

$$N_1 - N_2 = (1 - \epsilon_1) \cdot B_{\text{pn}} \quad (7)$$

Tab. IV shows the result of this test with background only. The values of  $N_1 - N_2$  from data is consistent, within errors, with Monte Carlo estimate of  $(1 - \epsilon_1)B_{\text{pn}}$ . Different selection cuts for the background yield similar results.

### IV. COMPARISON WITH “ON-OFF” BACKGROUND SUBTRACTION

The advantages of the swap method become clear in the comparison with the “ON-OFF” method, as shown in Tab. V. The Table summarizes the results of the Palo Verde experiment for the 1999 data taking period from [4].  $\epsilon_1$  is indeed very close to 1 resulting in a very small residual background  $(1 - \epsilon_1)B_{\text{pn}}$ , even for a background rate  $B_{\text{unc}} + B_{\text{nn}} + B_{\text{pn}}$  as high as  $27 \text{ d}^{-1}$ . In the new variable  $N_1 - N_2$ , not only the terms  $B_{\text{unc}}$  and  $B_{\text{nn}}$  drop completely, but also  $B_{\text{pn}}$  is strongly suppressed. A conservative 160% uncertainty on  $(1 - \epsilon_1)B_{\text{pn}}$  only corresponds to a 4% error on  $N_\nu$ . On the other hand,  $\epsilon_2$  is

	1999 “ON”	1999 “OFF”
No. of days	110.95	23.40
$\bar{\nu}_e$ efficiency	0.112	0.111
$\epsilon_2$	0.159	0.159
$(1 - \epsilon_1)B_{\text{pn}}$ , spall. in walls (d <sup>-1</sup> )	$-1.35 \pm 0.68$	$-1.33 \pm 0.67$
$(1 - \epsilon_1)B_{\text{pn}}$ , spall. in water (d <sup>-1</sup> )	-	-
$(1 - \epsilon_1)B_{\text{pn}}$ , capt. in walls (d <sup>-1</sup> )	$0.02 \pm 0.03$	$0.02 \pm 0.03$
$(1 - \epsilon_1)B_{\text{pn}}$ , capt. in water (d <sup>-1</sup> )	$0.86 \pm 0.43$	$0.86 \pm 0.43$
$N_1$ (d <sup>-1</sup> )	$52.9 \pm 0.7$	$43.9 \pm 1.4$
$N_2$ (d <sup>-1</sup> )	$32.3 \pm 0.5$	$31.7 \pm 1.2$
$N_\nu$ (d <sup>-1</sup> )	$25.2 \pm 0.9$	$15.1 \pm 1.9$
$B_{\text{unc}} + B_{\text{nn}} + B_{\text{pn}}$ (d <sup>-1</sup> )	$27.7 \pm 0.6$	$28.8 \pm 1.3$
$\bar{\nu}_e$ observed (d <sup>-1</sup> )	$225 \pm 8$	$136 \pm 17$
$\bar{\nu}_e$ expected (d <sup>-1</sup> )	218	130

TABLE V. Palo Verde results from 1999 data taking. Errors are statistical except for  $(1 - \epsilon_1)B_{\text{pn}}$  where errors are systematic. The individual background rates are approximately  $4 \text{ d}^{-1}$  for  $B_{\text{unc}}$ ,  $14 \text{ d}^{-1}$  for  $B_{\text{nn}}$  and  $10 \text{ d}^{-1}$  for  $B_{\text{pn}}$

only 0.16, small enough that the statistical power of the  $\bar{\nu}_e$  signal is retained.

Correcting  $N_1$  in both columns by their respective efficiencies and subtracting column 2 from column 1 in the Table, we find that the “ON-OFF” method gives a neutrino rate of  $77 \pm 14(\text{stat.}) \pm 8(\text{syst.}) \text{ d}^{-1}$  for an expectation of  $88 \text{ d}^{-1}$  in the no-oscillation hypothesis. In calculating the signal essentially only one reactor out of three is used, while the statistical fluctuations in the flux of all reactors along with the background contribute to the errors. The systematic error includes uncertainties on positron and neutron efficiencies (5%),  $\bar{\nu}_e$  selection (8%) and  $\bar{\nu}_e$  flux estimate (3%).

In the case of the swap method, we find  $225 \pm 8(\text{stat.}) \pm 17(\text{syst.}) \text{ d}^{-1}$  ( $137 \pm 17(\text{stat.}) \pm 14(\text{syst.}) \text{ d}^{-1}$ ) for high (low) power against a prediction of  $218 \text{ d}^{-1}$  ( $130 \text{ d}^{-1}$ ) for the case of no oscillations. Here all reactors contribute to the signal and, in fact, the contributions for the two periods with different power can be used together to strengthen the measurement. Indeed the statistical error drops from 18% in the case of “ON-OFF” to 3.5% (12%) for high (low) power. While systematic errors from efficiencies and flux are the same as in the previous case, the error on  $\bar{\nu}_e$  selection is now only 4% because some of the selection systematics cancel in the  $N_1 - N_2$  difference. A new uncertainty due to the  $B_{\text{pn}}$  estimate (4%) appears.

### V. SUMMARY AND DISCUSSIONS

We have shown that a novel method of analysis, applicable to low energy neutrino experiments using correlated signatures, provides substantially more accurate background subtraction over more traditional techniques. While the new method was applied first to a reactor neutrino oscillation experiment, it can be more generally

used in experiments where: a) the signal events consist of two sub-events correlated in time or space, b) the two sub-events are distinctively different from each other in signal but similar in backgrounds or vice-versa, and c) the detector and trigger treat the two sub-events in identical fashion.

These criteria apply to several future neutrino experiments such as KamLAND and LENS. In KamLAND [5] electron anti-neutrinos from reactors will be detected in 1 kton liquid scintillator as a positron with energy deposit between 1 and 8 MeV correlated in time with a neutron which gives a 2.2 MeV  $\gamma$  line from capture on protons. The correlated neutron background, which includes both one- and two-neutron events, is expected to have the same magnitude as the random background. The application of the method is therefore straightforward: both random and two-neutron backgrounds can be eliminated and the one-neutron background can be estimated in a way which is very similar to what we discussed above. The LENS experiment [3] is designed to detect solar neutrinos via, for example, the process  $\nu + {}^{160}\text{Gd} \rightarrow e^- + {}^{160}\text{Tb}^*$ , where the signature consists of an electron (0.04-2 MeV) and a  $\gamma$  (64 keV) correlated in time. One of the main backgrounds is the random coincidence of  $\gamma$ 's from radioactive impurities in the detector and it can be easily suppressed by the method described above.

## VI. ACKNOWLEDGMENTS

We would like to thank our Palo Verde collaborators for their continuing support and constructive criticism. Special thanks go to J. Busenitz for cross checks of the method's dependence on muon spallation models and P. Vogel for countless suggestions and advise. This work was supported in part by DoE grant DE-FG03-96ER40986. One of us (L.M.) would like to thank the ARCS foundation for its generous support.

- [8] M. Aglietta *et al.*, Nuovo Cim. 12C (1989) 467.
- [9] R. Hertenberger, M. Chen and B.L. Dougherty, Phys. Rev. 52C (1995) 2449.
- [10] J. Delorme *et al.*, Phys. Rev. C52 (1995) 2222.
- [11] O.G. Ryazhskaya and G.T. Zatsepin, Izv. Akad. Nauk USSR, Ser. Fiz., 29 (1965) 1946;  
O.G. Ryazhskaya and G.T. Zatsepin, Proceedings of the IX Inter. Conf. on Cosmic rays, Vol. 3, London, 1966, P.987.
- [12] O.C. Allkofer and R.D. Andresen, Nucl. Phys. B8 (1968) 402.
- [13] Karmen Collaboration, private communication.
- [14] J.C. Barton, Proceedings of the 19th Inter. Conf. on Cosmic rays, La Jolla, 1985, Physical Society, London, p. 98.
- [15] D.H. Perkins, "Calculation of neutron background in Soudan 2", unpublished, 1990.
- [16] G. Gratta *et al.*, Nucl. Instr. and Meth. A400 (1997) 456.
- [17] F. Boehm *et al.*, to be submitted to Phys. Rev. D.
- [18] R. Brun *et al.*, "GEANT 3", CERN DD/EE/84-1 (revised), 1987.
- [19] P.A. Aarnio *et al.*, "FLUKA user's guide", TIS-RP-190, CERN, 1990
- [20] T.A. Gabriel *et al.*, ORNL/TM-5619-mc, April 1977.
- [21] R.L. Craun and D.L. Smith, Nucl. Instr. and Meth. 80 (1970) 239.
- [22] F.F. Khalchukovet *al.*, Nuovo Cim. 6C (1983) 320.
- [23] K.V. Alanakyanet *al.*, Sov. J. Nucl. Phys. 34 (1981) 828.
- [24] T.K. Gaisser, "Cosmic Rays and Particle Physics", Cambridge University Press, 1990.
- [25] T. Suzuki *et al.*, Phys. Rev. 35C (1987) 2212.
- [26] R.B. Firestone, V.S. Shirley *et al.*, "Table of Isotopes", 8th Edition, Wiley Interscience, 1996.
- [27] N.C. Mukhopadhyay *et al.*, Phys. Rep. 30C (1977) 1.
- [28] E. Kolbe, K. Langanke and P. Vogel, Phys. Rev. 50C (1994) 2576.
- [29] P. Singer, "Springer tracts in Modern Physics", Vol. 71 (1974) 39.

- 
- [1] F. Reines and C.L. Cowan, Phys. Rev. 90 (1953) 90.
  - [2] See e.g. F. Boehm and P. Vogel, "Physics of Massive Neutrinos", Cambridge University Press 1992 (2<sup>nd</sup> Ed.).
  - [3] R.S. Raghavan, Phys. Rev. Lett. 78 (1997) 3618.
  - [4] F. Boehm *et al.*, submitted to Phys. Rev. Lett., preprint hep-ex/991250.
  - [5] P. Alivisatos *et al.*, "KamLAND Proposal", Preprint Stanford-HEP-98-03, Tohoku-RCNS-98-15, unpublished.
  - [6] See for example, Particle Data Group, "Review of Particle Physics", Euro. Phys. Jour. C3 (1998).
  - [7] M. Apollonio *et al.*, Phys. Lett. B420 (1998) 397;  
M. Apollonio *et al.*, Phys. Lett. B466 (1999) 415.